

## NUMERICAL CALCULATION OF THE FLOW REGIMES OF A FLUID PARTIALLY FILLING A HORIZONTAL ROTATING HEAT-EXCHANGE CYLINDER

Yu. V. Naumenko

UDC 532.516:518:517.9

*Consideration is given to a numerical determination of a two-dimensional unsteady viscous flow with the free surface in a stationarily rotating horizontal cylinder in which heat-exchange processes are carried out. The "marker-and-cell" method in a polar coordinate system is used. The features of modeling of the wall-layer regime and the circulating flow regime that occur in rapid and slow rotation of the cylinder, respectively, are discussed. Based on the given results of numerical calculations, the influence of the Reynolds number on the character of flow is analyzed.*

The problem of determination of a viscous flow with the free surface in a horizontal rotating cylinder is of significant applied interest for liquid horizontal rotary systems in which heat-exchange processes are carried out. The character of motion of a fluid governs the efficiency of realization of technological processes by rotating heat pipes, drying vapor cylinders, centrifugal casting machines, and other devices. Furthermore, the characteristics of the flow have an effect on the stability of the regimes of motion [1] and on the value of the moment of resistance of the fluid to the rotation of the cylinder (antitorque moment) [2].

Steady flow in stationary rotation of the cylinder is characterized by two regimes of motion [1]. The first regime in the form of an immobile wall quasi-annular layer occurs in rapid rotation of the cylinder. The second is realized in the form of combined circulating motion with considerable relative velocities and deformations of the free surface of a fluid and occurs in low-speed rotation.

The problem of determining the position of the free surface of a thin wall layer of the fluid in the first regime of motion was numerically solved in [3] based on the boundary-layer theory and with experimental check. Numerical approaches to determination of the flow in the form of a wall layer that are based on different methods are given in [4–7].

Because of the combined nature of the flow, the modeling of the second regime of motion is substantially complicated as compared to the description of the first regime. The results of experimental and to some extent theoretical investigations of the circulating regime of motion are given in [8–10]. Attempts at determining numerically the individual parameters of a circulating flow are presented in [11–13].

A characteristic feature of the problem in question is a complex geometry, large deformation of the free boundary, and mobility of a solid wall. However, in [3–7, 11–13], the modeling of such a flow using the existing simplified numerical methods fails to ensure the required accuracy. At the same time, rather wide acceptance has been gained by one of the most efficient algorithms for solution of nonstationary problems of flow with a complex shape of the free surface – the "marker-and-cell" (MAC) method [14]. The procedure initially developed for a rectangular Cartesian coordinate system was subsequently extended to a cylindrical system for the case of axial symmetry [15, 16]. The "marker-and-cell" method applied in polar coordinates that correspond most closely to the geometry of the flow and boundaries is used in [17] for a numerical solution of the two-dimensional nonstationary problem in question.

---

Rovno State Humanities University, Rovno, Ukraine. Translated from *Inzhenerno-Fizicheskii Zhurnal*, Vol. 74, No. 3, pp. 145–150, May–June, 2001. Original article submitted July 13, 2000; revision submitted November 20, 2000.

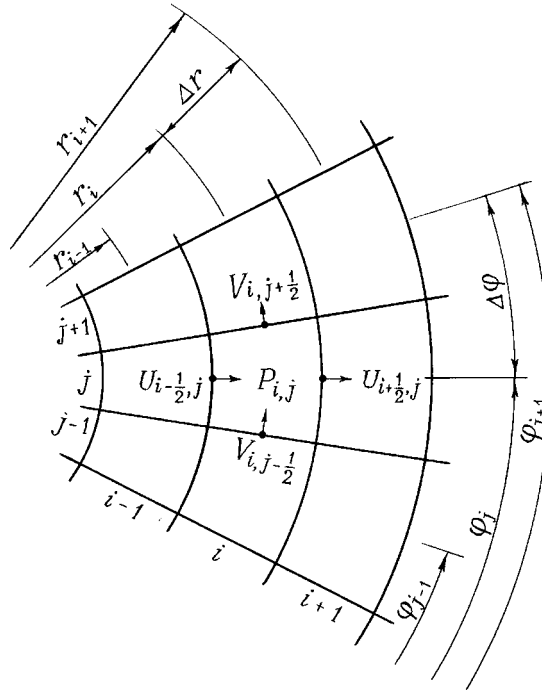


Fig. 1. Scheme of the computational grid.

The studied region of the circular cross section of a cylinder is covered with a polar grid of cells (Fig. 1). The velocity components are determined at the boundaries of the cell, while the pressure is determined at the center. Then, using finite-difference expressions for solution of Navier–Stokes equations in a conservative form in a polar coordinate system, we can obtain the following algorithm in dimensionless form:

$$U_{i+1/2,j}^{n+1} = F_{i+1/2,j}^n - \Delta t \frac{(P_{i+1,j} - P_{i,j})^{n+1}}{\Delta r}, \quad (1)$$

$$F_{i+1/2,j}^n = U_{i+1/2,j}^n + \Delta t \left\{ -\frac{(rU^2)_{i+1,j} - (rU^2)_{i,j}}{r_{i+1/2} \Delta r} - \frac{(UV)_{i+1/2,j+1/2} - (UV)_{i+1/2,j-1/2}}{r_{i+1/2} \Delta \varphi} + \left(\frac{V^2}{r}\right)_{i+1/2,j} - \frac{\sin \varphi_j}{\text{Fr}} + \frac{1}{\text{Re}} \left[ \frac{(rU)_{i+3/2,j} - (rU)_{i+1/2,j}}{r_{i+1}} - \frac{(rU)_{i+1/2,j} - (rU)_{i-1/2,j}}{r_i} \right] \frac{1}{\Delta r^2} + \frac{U_{i+1/2,j+1} - 2U_{i+1/2,j} + U_{i+1/2,j-1}}{r_{i+1/2}^2 \Delta \varphi^2} - \frac{2(V_{i+1/2,j+1/2} - V_{i+1/2,j-1/2})}{r_{i+1/2}^2 \Delta \varphi} \right\}^n, \quad (2)$$

$$V_{i,j+1/2}^{n+1} = G_{i,j+1/2}^n - \Delta t \frac{(P_{i,j+1} - P_{i,j})^{n+1}}{r_i \Delta \varphi}, \quad (3)$$

$$G_{i,j+1/2}^n = V_{i,j+1/2}^n + \Delta t \left\{ -\frac{(rUV)_{i+1/2,j+1/2} - (rUV)_{i-1/2,j+1/2}}{r_i \Delta r} - \frac{V_{i,j+1}^2 - V_{i,j}^2}{r_i \Delta \varphi} - \left(\frac{UV}{r}\right)_{i,j+1/2} - \frac{\cos \varphi_{j+1/2}}{\text{Fr}} + \right.$$

$$\begin{aligned}
& + \frac{1}{\text{Re}} \left\{ \frac{\left[ (rV)_{i+1,j+1/2} - (rV)_{i,j+1/2} \right] / r_{i+1/2} - \left[ (rV)_{i,j+1/2} - (rV)_{i-1,j+1/2} \right] / r_{i-1/2}}{\Delta r^2} + \right. \\
& \left. + \frac{V_{i,j+3/2} - 2V_{i,j+1/2} + V_{i,j-1/2}}{r_i^2 \Delta \phi^2} + \frac{2(U_{i,j+1} - U_{i,j})}{r_i^2 \Delta \phi} \right\}^n. \quad (4)
\end{aligned}$$

As the characteristic parameters we can adopt:  $R$ , length,  $\omega R$ , linear rotational velocity of the cylinder,  $\rho \omega^2 R^2$ , pressure on the surface of a filled cylinder in quasi-rigid-body rotation of the fluid, and  $1/\omega$ , time of rotation of the cylinder by one radian.

The finite-difference approximation of the continuity equation has the form

$$D_{i,j}^{n+1} = \left[ \frac{(rU)_{i+1/2,j} - (rU)_{i-1/2,j}}{r_i \Delta r} + \frac{V_{i,j+1/2} - V_{i,j-1/2}}{r_i \Delta \phi} \right]^{n+1} = 0. \quad (5)$$

The substitution of the velocity components from Eqs. (1) and (3) makes it possible to represent (5) in the form of a difference Poisson equation for pressure in polar coordinates:

$$\begin{aligned}
& \left[ \frac{r_{i+1/2} (P_{i+1,j} - P_{i,j}) - r_{i-1/2} (P_{i,j} - P_{i-1,j})}{r_i \Delta r^2} + \frac{P_{i,j+1} - 2P_{i,j} + P_{i,j-1}}{r_i^2 \Delta \phi^2} \right]^{n+1} = \\
& = \frac{1}{\Delta t} \left[ \frac{(rF)_{i+1/2,j} - (rF)_{i-1/2,j}}{r_i \Delta r} + \frac{G_{i,j+1/2} - G_{i,j-1/2}}{r_i \Delta \phi} \right]^n. \quad (6)
\end{aligned}$$

With account for (2) and (4), the right-hand side of Eq. (6) can be written in the form

$$\begin{aligned}
& \frac{1}{\Delta t} \left[ \frac{(rF)_{i+1/2,j} - (rF)_{i-1/2,j}}{r_i \Delta r} + \frac{G_{i,j+1/2} - G_{i,j-1/2}}{r_i \Delta \phi} \right]^n = \frac{D_{i,j}^n}{\Delta t} - L_{i,j}^n, \quad (7) \\
& L_{i,j}^n = \left\{ \frac{(rU^2)_{i+1,j} - 2(rU^2)_{i,j} + (rU^2)_{i-1,j}}{r_i \Delta r^2} + \right. \\
& + \frac{(UV)_{i+1/2,j+1/2} - (UV)_{i+1/2,j-1/2} - (UV)_{i-1/2,j+1/2} + (UV)_{i-1/2,j-1/2}}{r_i \Delta r \Delta \phi} + \\
& + \frac{r_{i+1/2} [(UV)_{i+1/2,j+1/2} - (UV)_{i+1/2,j-1/2}] - r_{i-1/2} [(UV)_{i-1/2,j+1/2} - (UV)_{i-1/2,j-1/2}]}{r_i^2 \Delta r \Delta \phi} + \\
& + \frac{V_{i,j+1}^2 - 2V_{i,j}^2 + V_{i,j-1}^2}{r_i^2 \Delta \phi^2} - \frac{V_{i+1/2,j}^2 - V_{i-1/2,j}^2}{r_i \Delta r} + \frac{(UV)_{i,j+1/2} - (UV)_{i,j-1/2}}{r_i^2 \Delta \phi} - \\
& \left. - \frac{1}{\text{Re}} \left[ \frac{r_{i+1/2} (D_{i+1,j} - D_{i,j}) - r_{i-1/2} (D_{i,j} - D_{i-1,j})}{r_i \Delta r^2} + \frac{D_{i,j+1} - 2D_{i,j} + D_{i,j-1}}{r_i^2 \Delta \phi^2} \right] \right\}^n.
\end{aligned}$$

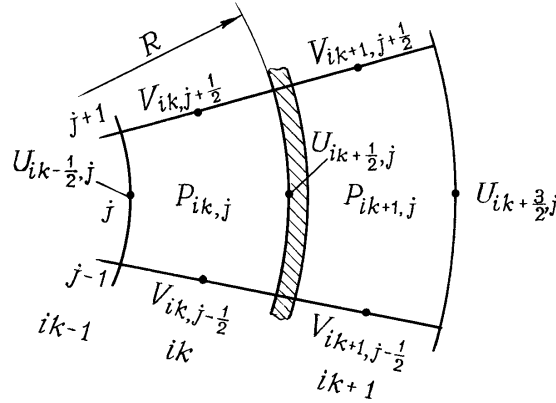


Fig. 2. Layer of fictitious cells.

For the boundary conditions on the solid wall to be realized, the polar grid is supplemented with an annular layer of fictitious cells located behind the boundary of the calculated region (Fig. 2). From the adhesion condition on the solid wall we have

$$U_{ik+1/2} = 0, \quad (8)$$

$$V_{ik+1/2} = \omega R = 1. \quad (9)$$

With account for (9), the expression for the tangential component of the velocity in a fictitious cell has the form

$$V_{ik+1,j+1/2} = 2 - V_{ik,j+1/2}. \quad (10)$$

Having written (5) for boundary and fictitious cells and adding these equations together with account for (8) and (9), upon rearrangements we obtain the expression for the radial component of the velocity in a fictitious cell:

$$U_{ik+3/2,j} = U_{ik-1/2,j} \frac{1 - \Delta r}{1 + \Delta r}. \quad (11)$$

Having used (1) and (2) for the wall surface with account for (8)–(11), we represent, upon rearrangements, the expression for the pressure in a fictitious cell in the form

$$P_{ik+1,j} = P_{ik,j} + \Delta r + \frac{2U_{ik-1/2,j}}{\text{Re } \Delta r} \frac{1 - \Delta r}{1 - (\Delta r/2)^2}. \quad (12)$$

The velocity components in surface cells adjacent to the free surface are found by extrapolation using the velocities in neighboring filled cells. The value of the pressure at the center of a surface cell is determined by interpolation of the pressure in one of the neighboring filled cells and the zero pressure on the free surface (Fig. 3) from the formulas

$$P_{ij} = P_{i+1,j} \left( 1 - \frac{\Delta r}{r_i + \Delta r - r_s} \right) \quad (13)$$

or

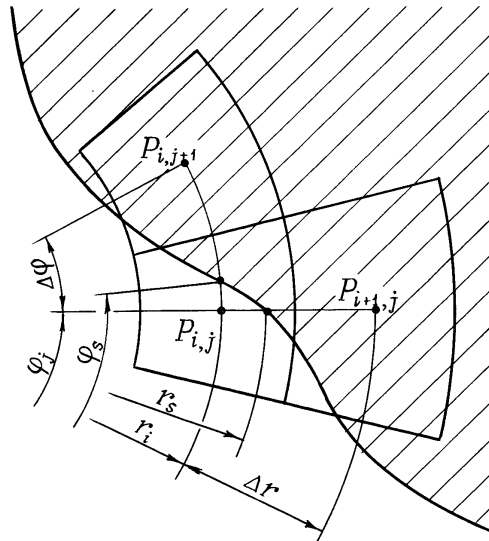


Fig. 3. Interpolation of pressure in a surface cell.

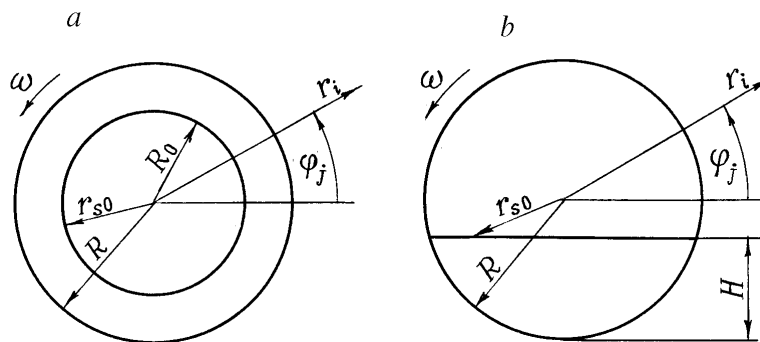


Fig. 4. Initial conditions from infinitely rapid rotation (a) and from the state of rest (b).

$$P_{i,j} = P_{i,j+1} \left( 1 - \frac{\Delta\varphi}{\varphi_j + \Delta\varphi - \varphi_s} \right). \quad (14)$$

In calculating the flow regimes, we set two variants of boundary conditions.

In the first case, it was assumed at the initial instant of time that  $\omega_0 = \infty$  and the fluid is rotating together with the cylinder as a rigid body and occupies the annular region in the cross section (Fig. 4a). Then the initial conditions for the free surface and the values of the velocity and pressure fields for the region occupied by the fluid become, in dimensionless form,

$$r_{s0} = \frac{R_0}{R}; \quad U_{i,j} \equiv 0; \quad V_{i,j} = r_i, \quad P_{i,j} = \frac{r_i^2 - r_{s0}^2}{2}. \quad (15)$$

In the second case, it was assumed that  $\omega_0 = 0$  and the fluid is at rest and, in the cross section, occupies the segment region in the lower part of the cavity (Fig. 4b). Then the analogous boundary conditions will be represented as

$$r_{s0} = \frac{H - R}{R \sin \varphi_j}; \quad U_{i,j} = V_{i,j} \equiv 0; \quad P_{i,j} = \frac{\frac{H - R}{R} - r_i \sin \varphi_j}{Fr}. \quad (16)$$

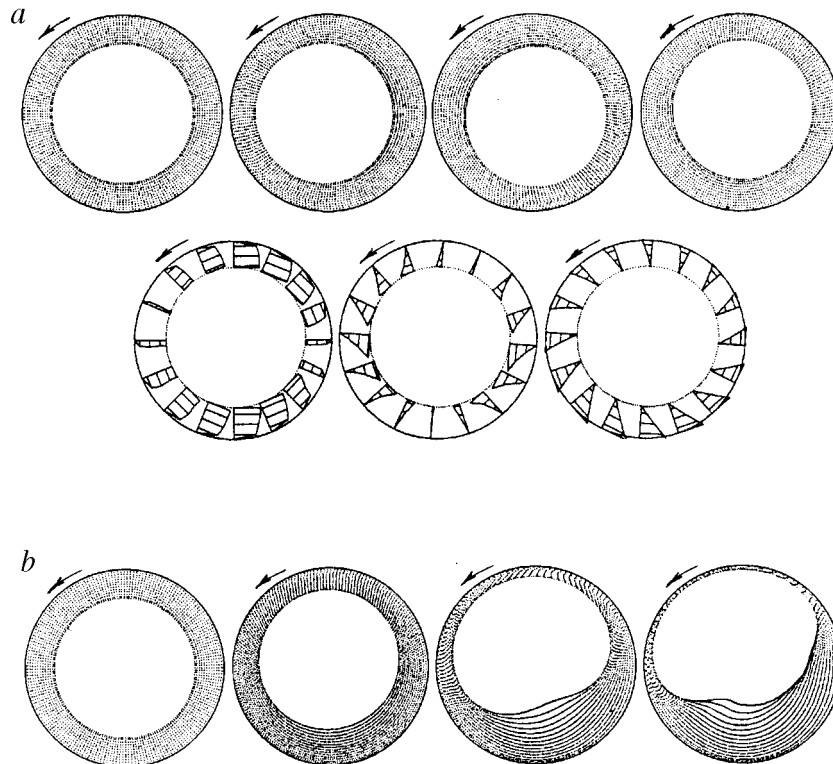


Fig. 5. Calculation of the flow with  $Re = 133,000$ ,  $Fr = 4.24$ , and  $\kappa = 0.5$  for  $t = 0, 10.1, 20.2$ , and  $30.3$ : a) patterns of the wall-layer regime and the  $V_{rel}$ ,  $U$ , and  $P$  diagrams for  $t = 30.3$ ; b) patterns of the circulating regime.

The computational process upon setting the initial conditions (15) or (16) consisted of the time steps and the cycles. The calculational cycle for a single time layer involved the following stages:

- 1) calculation of the pressure field from (6) with account for (7) and (1)–(4), and also from (12) and (13) or (14);
- 2) calculation of the velocity field from (1)–(4), (10), and (11);
- 3) calculation of new coordinates of the markers upon movement and of a new position of the free surface;
- 4) refinement of the velocity and pressure fields near the boundary;
- 5) passage to a new time layer and a new calculational cycle.

The stable numerical solution was ensured by an accurate determination of the pressure field with the attainment of the convergence criterion assigned in advance. In realization of the method, most of the computer time was consumed by this calculation. The Poisson equation for pressure was solved by the Gauss–Seidel iteration method with successive overrelaxation. The optimum value of the relaxation parameter was determined experimentally and was equal to 1.5–1.8.

In calculating the regime of flow in the form of a wall layer, the initial conditions (15) were used. Figure 5a shows successive patterns of development of this regime with the degree of filling of the cylinder  $\kappa = 0.5$  for four instants of time and diagrams of, respectively, the relative tangential  $V_{rel} = V - 1$  and absolute radial  $U$  velocity and the pressure  $P$  for the last pattern (in the case of coincidence of the diagram's ordinate with the direction of rotation, its value is positive). The value of the maximum ordinate was 0.0493 for the  $V_{rel}$  diagram, 0.0196 for the  $U$  diagram, and 0.373 for the  $P$  diagram.

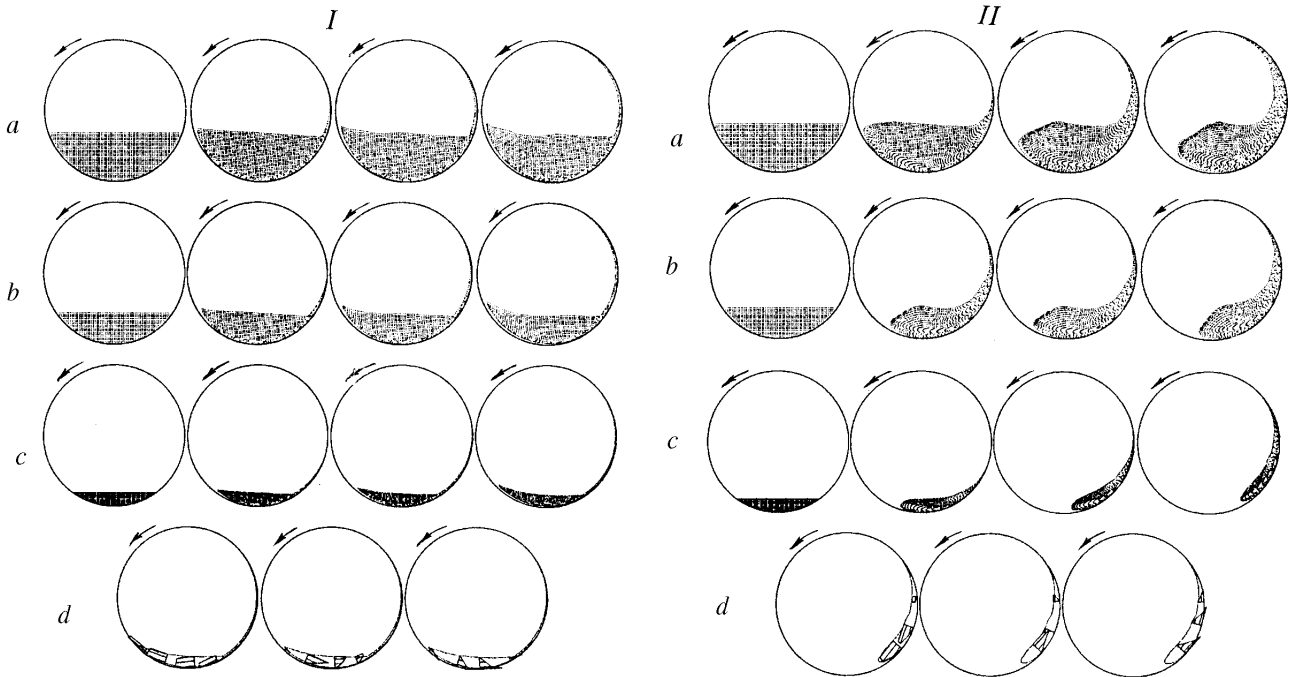


Fig. 6. Calculation of the circulating regime of flow with  $Re = 225,000$  (*I*),  $Re = 1125$  (*II*), and  $Fr = 3.06$  for  $t = 0, 0.57, 1.13,$  and  $1.17$ : the patterns with  $\kappa = 0.3$  (*a*),  $\kappa = 0.15$  (*b*), and  $\kappa = 0.05$  (*c*) and the  $V_{rel}$ ,  $U$ , and  $P$  diagrams (*d*) with  $\kappa = 0.05$  for  $t = 1.17$ .

The diagrams of the velocity components in Fig. 5a demonstrate the acceleration of the descending part of the annular cross section of the layer and the retardation of the ascending part. The flow patterns show a marked variable wall thickness of the layer that varies in the process of development of the flow.

As the rotational velocity decreases to a value lower than the limiting one for which the wall-layer regime changes to a circulating regime during the retardation of the cylinder [1], the convergence of the iteration computational process decreased sharply. Recording of the manifestation of this instability was used for a numerical determination of the value of the indicated lower limiting velocity in changeover of the regimes.

The complicated character of the circulating regime of flow as compared to the wall-layer regime motivates the necessity of improving the accuracy of determination of the velocity components and the pressure on the free surface for ensuring the stability of the calculational scheme [18]. In order to calculate such a regime, we can also use conditions (15), assuming that the rotation of the cylinder is slow as compared to rapid relative motion of the fluid. Figure 5b shows the patterns of development of the regime under these conditions for parameters of the flow that correspond to those of Fig. 5a. However, such initial conditions ensure the stability of the solution only when the initial wall-layer regime in the case of a rotational velocity no lower than the limiting one exists. Furthermore, despite the relative simplicity, these conditions introduce specific distortions into the position of the free surface.

For a more accurate calculation of the circulating regime we used conditions (16). Figure 6 *I* shows the patterns of development of the regime using similar conditions with large Reynolds numbers for three degrees of filling of the cylinder. The value of the maximum ordinate for the last pattern was 1.14 for the  $V_{rel}$  diagram, 0.02 for the  $U$  diagram, and 0.0909 for the  $P$  diagram. Figure 6 *II* gives the pattern of development of such a regime with small  $Re$  for flow parameters that correspond to the parameters of Fig. 6 *I*. For the last pattern, the value of the maximum ordinate was 0.327 for the  $V_{rel}$  diagram, 0.0262 for  $U$ , and 0.131 for  $P$ .

According to the flow patterns in Fig. 6 I, practically the entire fluid in weak interaction with the wall of the cylinder, even for a low degree of its filling, is found in the lower part of the cavity with a nearly horizontal free surface; the fluid slips past the cylinder, and just its thin layer adheres to the ascending part of the wall. According to the patterns in Fig. 6 II, in strong interaction with the cylinder, the bulk of the fluid executes an intense circulating motion with the formation of a vortex roller on the descending part of the wall and a meniscus with a considerable adherent layer on the ascending part. When the degree of filling is low the fluid in the cross section becomes drop-shaped, fails to slip past the wall (due to the strong adhesion), and spreads over it.

Consequently, use of the initial conditions (16) instead of conditions (15) improves the accuracy of determination of the position of the free surface in circulating flow. The velocity range of solution is also extended, since the convergence of a computational process decreases substantially only when the rotational velocity increases to the upper limiting value for which the circulating regime changes to a wall-layer regime in the acceleration of the cylinder [1]. Recording of such instability was also used for a numerical determination of the value of the upper limiting rotational velocity of the cylinder.

In solving the two problems of determination of the flow regimes, we carried out control calculations that showed a good approximal convergence and algorithmic universality of the method. With the aim of monitoring the computations, we also checked the fulfillment of the condition of conservation of mass. The error was insignificant.

Thus, the "marker-and-cell" method employed in polar coordinates is applicable to modeling the entire class of the considered flows with the free surface. The procedure makes it possible to carry out a qualitative numerical analysis of the character and boundaries of changeover of combined regimes of flow in a horizontal rotating cylinder and based on this to predict with a sufficient degree of reliability the technological parameters of liquid horizontal drum heat-exchange systems.

## NOTATION

$r$  and  $\varphi$ , radial and angular coordinates;  $U$  and  $V$ , radial and tangential components of the velocity;  $D$ , divergence of the velocity;  $P$ , pressure;  $t$ , time;  $\nu$ , kinematic coefficient of viscosity;  $\rho$ , density;  $\Delta r$  and  $\Delta\varphi$ , sides of the annular sector of the polar grid's cell;  $R$ , cylinder radius;  $\omega$ , angular velocity of the cylinder;  $g$ , gravitational acceleration;  $Re = \omega R^2/\nu$ , Reynolds number;  $Fr = \omega^2 R/g$ , Froude number;  $\Delta t$ , time step;  $n$  and  $n + 1$ , number of the time cycle;  $G$ ,  $F$ , and  $L$ , variables;  $r_s$  and  $\varphi_s$ , coordinates of the points of intersection of the free boundary and the radial and arc segments that connect the centers of the surface cell and the filled cell;  $\omega_0$ , angular velocity of the cylinder at the initial instant of time;  $R_0$ , radius of the free surface of the fluid in infinitely rapid rotation of the cylinder;  $r_{s0}$ , radial coordinate of the free surface at the initial instant of time;  $H$ , height of the segment layer of the fluid at rest;  $\kappa$ , degree of filling of the cylinder with the fluid;  $V_{rel}$ , relative tangential velocity. Subscripts:  $i$  and  $j$ , radial and angular coordinates of the center of the cell;  $k$ , radial coordinate of the cylinder wall;  $s$ , coordinate of the free surface;  $0$ , value of the parameter at the initial instant of time;  $rel$ , relative velocity.

## REFERENCES

1. Yu. V. Naumenko, *Inzh.-Fiz. Zh.*, **64**, No. 5, 558–565 (1993).
2. Yu. V. Naumenko, *Inzh.-Fiz. Zh.*, **71**, No. 4, 639–642 (1998).
3. J. A. Deiber and R. L. Cerro, *Ind. Eng. Chem., Fundam.*, **15**, No. 2, 102–110 (1976).
4. K. J. Ruschak and L. E. Scriven, *J. Fluid Mech.*, **76**, No. 1, 113–125 (1976).
5. F. M. Orr and L. E. Scriven, *J. Fluid Mech.*, **84**, No. 1, 145–165 (1998).
6. R. F. Gans, *J. Fluid Mech.*, **82**, No. 3, 415–427 (1977).



7. R. F. Gans, *J. Fluid Mech.*, **93**, No. 3, 529–548 (1979).
8. J. Gavish, R. S. Chadwick, and C. Gutfinger, *Isr. J. Technol.*, **96**, Nos. 5–6, 264–272 (1978).
9. Y. Suzuki and Y. Tanida, in: *Proc. 3rd Asian Symp. Visual.*, Tokyo (1994), pp. 230–235.
10. K. A. Jackson, J. E. Finck, C. R. Bednarski, and L. R. Clifford, *Amer. J. Phys.*, **64**, No. 3, 277–282 (1996).
11. A. Haji-Sheikh, R. Lakshimanarayanan, D. Y. S. Lou, and P. J. Ryan, *Trans. ASME, J. Fluids Eng.*, **106**, No. 3, 270–278 (1984).
12. S. A. Trusov, V. I. Lapitskii, V. V. Vachevskikh, and L. K. Filimonova, in: *Rheology and Processes and Apparatuses of Chemical Engineering* [in Russian], Volgograd (1989), pp. 71–77.
13. V. A. Yakutenok, *Mat. Modelir.*, **4**, No. 10, 62–70 (1992).
14. F. H. Harlow and J. E. Welch, *Phys. Fluids*, **8**, No. 12, 2182–2189 (1965).
15. F. H. Harlow and J. P. Shannon, *Science*, **157**, No. 3788, 547–550 (1967).
16. B. J. Daly, *Phys. Fluids*, **12**, No. 7, 1340–1354 (1969).
17. Yu. V. Naumenko, *Zh. Vychisl. Mat. Mat. Fiz.*, **39**, No. 2, 294–299 (1999).
18. B. D. Nichols and C. W. Hirt, *J. Comput. Phys.*, **8**, No. 3, 434–448 (1971).